6
Solidification and melting along dykes by the laminar flow of basaltic magma

Paul M. Bruce* **and Herbert E. Huppert**
Department of Applied Mathematics and Theoretical Physics,
University of Cambridge,
Silver Street,
Cambridge CB3 9EW, UK

Abstract

We model the important thermal effects that occur when hot basaltic magma flows through a newly opened dyke during an eruption. Heat is advected along the dyke by the flowing magma and simultaneously is lost from the dyke by conduction into the colder crustal rock surrounding the dyke. During the early stages of the eruption, the conductive heat losses are dominant and the dyke becomes constricted due to the solidification of magma against the walls. Solidification occurs preferentially at the downstream end of the dyke near the surface and the dyke may become completely blocked at the surface. The eruption at that site will then cease before the supply of magma has been exhausted. Alternatively, in dykes with an initial width that is sufficiently large, the continual supply of heat by the flowing magma may, after a time, exceed the heat losses into the surrounding country rock. In these cases the initial solidification is reversed, the walls of the dyke are progressively melted, and the dyke is widened until the supply diminishes. We carry out explicit calculations for a two-dimensional dyke. The results are that for typical physical parameters for basaltic magmas the initial critical width that demarcates these two regimes is of the order of 1 m and is a strong function of the initial temperature of the surrounding country rock. When the physical processes revealed by our two-dimensional model are extrapolated to three dimensions, we identify an intermediate regime. For dykes with an initial width close to the critical value, cross flows within the dyke lead to only parts of the surface becoming blocked. This indicates how an eruption from an initially long surface fissure can become confined to a number of isolated vents after a while.

Contents

Notation

		Units
K	normalized dimensionless solidification rate	
L	latent heat of either solidification or melting	J kg^{-1}
Q	volume flow rate in dyke	m^3 s^{-1}
S_m	Stefan number of fluid magma	
S_∞	Stefan number of solid rock	
T	dimensionless time	
T_w	temperature at the edge of the dyke	°C

* Present address: Shell International Petroleum Co. Ltd, Shell Centre, London SE1 7NA, UK

Magma Transport and Storage. Edited by M.P. Ryan

T_m	temperature of magma at the base and in the interior of the dyke	°C
T_∞	far-field temperature in the country rock	°C
V	dimensionless velocity of dyke wall	
X	dimensionless local coordinate axis perpendicular to dyke wall	
Z	dimensionless local coordinate axis along dyke wall	
Z_h	dimensionless coordinate at top of dyke	
b	half-width of dyke	m
b_i	initial half-width of dyke	m
c	specific heat	$J\,kg^{-1}\,°C^{-1}$
h	length of dyke	m
l_c	conductive length-scale	m
t	time	s
v	velocity of dyke wall	$m\,s^{-1}$
w	velocity scale of magmatic flow	$m\,s^{-1}$
x	local coordinate axis perpendicular to dyke wall	m
y	dummy variable	
z	local coordinate axis along dyke wall	m
Γ	ratio of shear to its initial value	
Γ_h	ratio of shear at top of dyke to its initial value	
ΔP	excess reservoir pressure	$N\,m^{-2}$
α	ratio of initial width of thermal boundary layer at top of dyke to the initial half-width	
γ	magnitude of shear	s^{-1}
γ_i	initial magnitude of shear in dyke of uniform width	s^{-1}
η	similarity variable	
θ	temperature in both magma and surrounding country rock	°C
ϑ	dimensionless temperature in magma	
$\varkappa$	thermal diffusivity	$m^2\,s^{-1}$
μ	Newtonian dynamic viscosity	Pa s
ξ	similarity variable	
ξ_0	specific value of similarity variable	
τ	similarity variable	
τ_d	demarcation value of τ	
ϕ	dimensionless temperature in surrounding country rock	

Introduction

Basaltic magma chambers can store large amounts of magma just a few kilometres beneath the Earth's surface. An increase in pressure in the chamber, due either to fluid and thermal processes within the chamber or to large-scale tectonic movement, can cause the magma to be extruded on to the Earth's surface. The magma is transported through the crust in a complicated series of dyke fractures that propagate both upwards and sideways from the chamber. Wherever a dyke reaches the surface, an eruption occurs, and for some time magma flows directly from the magma chamber to the surface. Thermal controls on the magma as it flows through the dyke play an essential role in determining the development and duration of the eruption. An investigation of the fundamental fluid and thermal processes that occur in basaltic dykes is the major aim of this chapter.

Volcanic eruptions of basaltic magma display a range of fascinating behaviours, which to date are only superficially understood. Due to their relatively low viscosity and volatile content, basaltic magmas tend to be extruded in non-explosive eruptions. The general behaviour of Hawaiian volcanism has been described by Macdonald and Abbot (1970) and summarized by Delaney and Pollard (1982). Figures 1 and 2 present colour photographs of the surface manifestations of a number of such Hawaiian eruptions. The eruptions typically commence with a linear system of fissures, often in an en echelon pattern, as seen in Figures 1 and 2. The fissures rapidly open at the surface and erupt a continuous fountain of lava in a 'curtain of fire', as is seen so clearly in the figures. The subsequent development varies from eruption to eruption. In some cases the height of the curtain of fire and the flow rate decrease and the eruption ceases, generally within a fraction of a day. In other eruptions, after a few hours a second phase is gradually initiated in which there is a decrease in the length of active fissures accompanied by a concentration of the height of fountaining at certain points along the

fissure. If the eruption continues, the flow of lava can become localized to only a few surface vents, around which volcanic cones are gradually built up.

This sequence of events was observed and fully documented in the 1959 eruption of Kilauea Iki, Hawaii, by Richter *et al.* (1970). An initial system of six fissures rapidly evolved to occupy a surface length of 750 m. After 2 h the extrusions of lava had become localized to one or two vents along each fissure and after 24 h the eruption was confined to a single vent. Over the following 35 days a substantial pyroclastic cone developed, which covered the initial fissure system. Further examples come from the Icelandic eruptions of Krafla between 1975 and 1984 (e.g., Björnsson *et al.*, 1979) and Heimay in 1973 (Thorarinsson *et al.*, 1973). At Krafla a multitude of short-lived eruptions occurred and each gradually declined in strength and eventually ceased after a few days. At Heimay the initial opening of a fissure 1.5 km long was rapidly followed by eruptions along its entire length. Ten hours after the commencement of the eruption, lava fountaining was increasingly concentrated at the middle of the fissure and, while the eruptive activity decreased in strength over the first few days, the eruption continued for several months. The eruption of Laki in 1783, the most voluminous historical eruption, led to dozens of vents along a fissure 15 km long that continually discharged lava (Thorarinsson, 1969).

Aside from the initial geometry, two effects control the rate and duration of discharge of magma from the chamber to the surface. The first is the driving pressure in the reservoir and the second is the thermal evolution of the magma and the country rock through which it passes. As the eruption continues, the driving pressure gradually decreases and may reduce the flow rate. The magnitude of this effect will generally be small, however, because it reflects the generally small fraction of the magma contained in the chamber that is ultimately erupted. An additional consequence of the decreasing pressure in the chamber is the tendency for the fluid withdrawal to produce subsidence of the chamber roof and to close the dykes emanating from the chamber. This may be the final limiting factor for some sustained eruptions. The second effect, thermal evolution, will play an important role throughout the eruption. As the hot basaltic magma rises in a newly opened dyke surrounded by relatively colder country rock, two important transfers of thermal energy occur. The first is the advection of heat by the magma as it flows along the dyke. The second is the conduction of heat out of the dyke into the colder surroundings. When magma first fills the dyke it initially solidifies against the cold channel walls. Continued solidification may eventually block the channel, which tends to end the eruption at that site even though the driving pressure in the magma chamber may remain substantial. However, the continual supply of heat to the walls by the magma flowing from the chamber may eventually exceed the possible conductive transfer into the country rock. Initial solidification will then be halted and the walls subsequently melted. The dyke width thus continues to increase until the magma supply diminishes. A similar scenario for initial solidification followed by melting was quantitatively analysed by Huppert (1989) for the turbulent flow in Archaean komatiite lavas over their solid floor rocks.

The calculations in the present study are for a simple two-dimensional model of a basaltic dyke. They evaluate the conditions under which melting can occur or, alternatively, the time for the eruption to cease if the dyke becomes blocked by continued solidification. In addition, we identify and explain an intermediate regime that can occur in a real three-dimensional dyke, whereby parts of the surface fissure become blocked and the eruption continues at a number of isolated vents due to cross flows within the dyke.

Description of the Model

An analysis of the evolution of magma in a dyke based solely on conductive transfers from the magma to the surrounding country rock implicitly assumes that static solidification of the magma is the only process that can occur. The flow will cease within a few days if the dyke is less than about a metre or so wide (Carslaw and Jaeger, 1959; Jaeger, 1968). A two-dimensional model of a dyke that incorporated advective transfers (Delaney and Pollard, 1982) allowed in principle for melting of the surrounding crust to occur, but concluded that in practice only solidification is geologically relevant. However, the model is incomplete in that it neglects both the effects of latent heat release on solidification and the influence of thermal advection in the magma on the

temperature profile in the solid. These deficiencies led the model to consistently overestimate the tendency for the dyke to become blocked. Our model builds on that of Delaney and Pollard and includes the effects they neglected. This permits us to describe theoretically for the first time how meltback of the walls of a basaltic dyke can occur and how this process allows a fissure eruption to continue.

We shall not consider here the initial formation of a dyke—a problem in solid mechanics that is still incompletely understood (Spence and Sharp, 1985; Lister, 1990). Our point of commencement is a two-dimensional dyke of initially uniform width that subsequently changes owing to local solidification or melting, as sketched in Figure 3. As the magma in the thin thermal boundary layer adjacent to the wall is cooled, its physical parameters can change quite drastically, as outlined, for example, by McBirney and Murase (1984). However, the transition between fluid magma and an effectively immobile crystal mush occurs within a layer in which the thickness is very much less than the width of the dyke. The time taken for the main part of the magma to travel the length of the dyke is rather less that an hour, and so, even at moderate undercooling, homogeneous nucleation produces little crystallization (Brandeis and Jaupart, 1986). We thus assume that the magma within the flowing thermal boundary layer at the walls of the dyke can be described as a Newtonian fluid of uniform viscosity, μ, which we shall, for definiteness, take as 100 Pa s (see, e.g., Ryan and Blevins, 1987). With this viscosity and with typical dyke widths of the order of 1 m and flow rates of less than a few metres per second, the motion is laminar and the velocity profile is given by the well-known parabolic Poiseuille law. We assume that this flow is driven by a constant excess pressure in the reservoir, ΔP. This assumption of a constant pressure, rather than the less appropriate, though frequently used, constraint of a constant flow rate, means that the magma velocity and flow rate realistically decrease as the dyke becomes constricted. We neglect any effects due to viscous heating (see, e.g., Hardee and Larson,

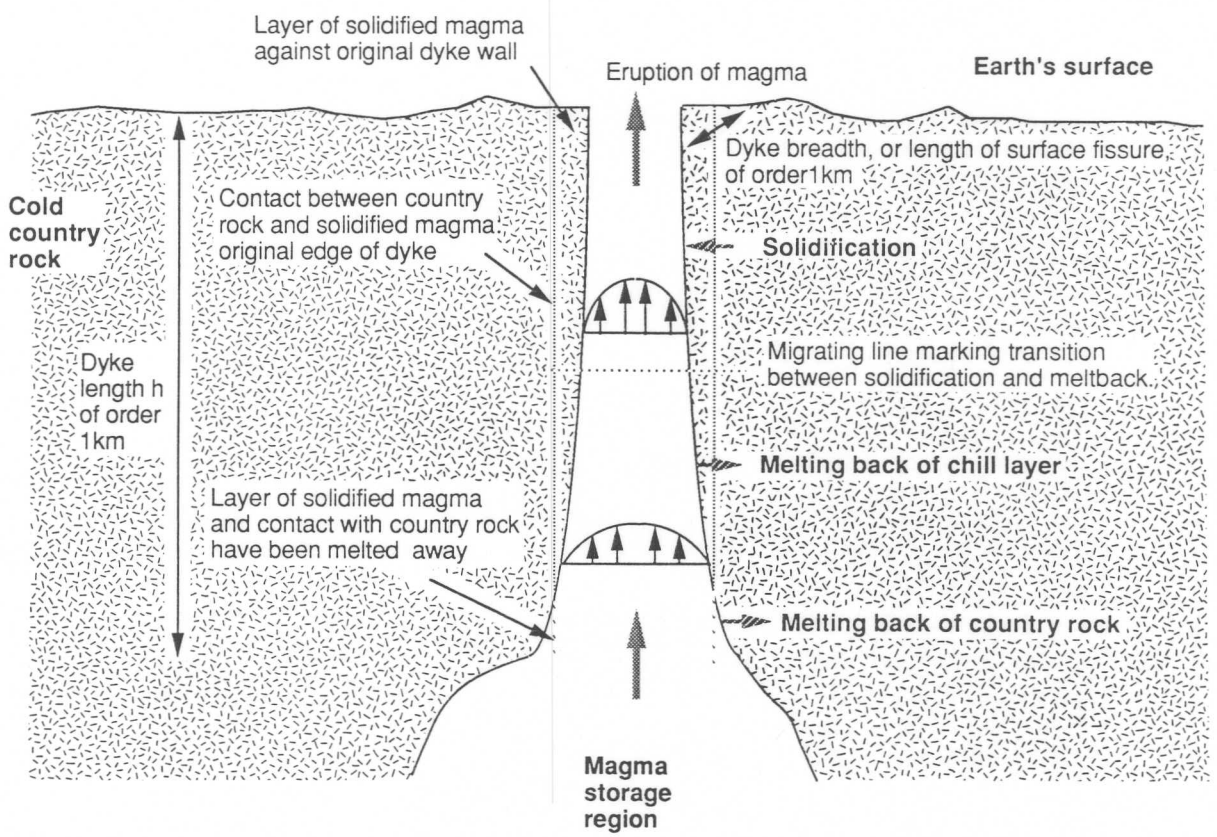

Figure 3. Cross-section through a typical sheet-like planar dyke. Note that the dyke need not necessarily be vertical

1977), which are negligible except possibly in dykes with a width that is very much larger than those we calculate to be at the critical value.

The temperature at the wall is taken to be fixed at T_w, which we identify as that temperature at which there is a transition between relatively fast flowing supercooled magma and a viscous, immobile crystal slurry. In reality the transition occurs over a temperature range. This range tends to be small, however, when compared with the difference between T_w and T_∞, the far-field temperature in the country rocks surrounding the dyke, and will hence be neglected.

The time taken for magma in the main dyke flow to traverse a dyke of length h is h/w, where w is the velocity scale of the flow. In this time thermal conduction is effective over a length-scale $l_c = (\varkappa h/w)^{1/2}$, where $\varkappa$ is the thermal diffusivity. With $\varkappa = 10^{-6}\ \mathrm{m^2\ s^{-1}}$, $h = 2 \times 10^3$ m and $w = 1\ \mathrm{m\ s^{-1}}$, $l_c \sim 4$ cm. Thus, l_c is typically very much less than both the length and the width of a dyke. The former inequality indicates that thermal conduction along the dyke can be neglected with respect to thermal advection by the main flow. The latter indicates that conduction across the dyke is only important in the thin thermal boundary layers adjacent to the walls.* Within these boundary layers the main Poiseuille flow appears as a uniform shear flow with a velocity that increases linearly from zero at the wall. The width of the dyke, the thermal boundary layers at the walls and the magnitude of the velocity shear across them will vary gradually along the dyke and slowly with time.

An important input into the model is the far-field temperature in the crust, T_∞. The appropriate value is set by any pre-heating that may have been caused by previous eruptions and by the possible presence of hydrothermal motions before the eruption (hydrothermal motion during the eruption plays virtually no role, as shown by Delaney (1982)). The value of T_∞ is one of the major external parameters used in the model.

The next section explains the details of the mathematical model and the following section presents the results of our numerical calculations. Thus readers who are interested in the results but not the mathematical details of our work could proceed directly to the section giving the results.

* We shall see later that it is the velocity scale at the edge of the boundary layer, rather than the core flow, which is important in determining the width of the thermal boundary layer. This width is typically of the order of 10 cm at the top of the dyke.

The Quantitative Calculations

Our model assumes that at time $t = 0$ a dyke of uniform width is instantaneously emplaced and a flow is initiated along the dyke. Within each thermal boundary layer a shear flow of magnitude γ flows along a wall of height h, which is at temperature T_w. The wall migrates into the flow with velocity v due either to the solidification of the flow against the wall ($v > 0$) or to melting of the wall by the flow ($v < 0$). The fluid at the start of the wall and outside the thermal boundary layer is at temperature T_m. Heat is transported in the fluid either by conduction across the flow or advection along it. With respect to locally cartesian coordinates, z measured along the wall and x perpendicular to it with $x = 0$ at the wall, as sketched in Figure 4, the governing partial differential equation for the temperature in the fluid $\theta(x, z, t)$, is

$$\theta_t - v\theta_x + \gamma x\theta_z = \varkappa\theta_{xx} \qquad (x, t > 0) \qquad (1)$$

$$\theta = T_m \qquad (z = 0) \qquad (2a)$$

$$\theta = T_w \qquad (x = 0) \qquad (2b)$$

$$\theta = T_m \qquad (x \to \infty) \qquad (2c)$$

and

$$\theta = T_m \qquad (t = 0) \qquad (2d)$$

where $\varkappa$ is the thermal diffusivity and (2d) indicates that all the fluid is initially at temperature T_m.

In the solid, heat is transported by conduction away from the wall. Initially throughout the solid and at all times far from the wall the temperature is assumed to be T_∞. The partial differential equation for the temperature in the solid is thus

$$\theta_t - v\theta_x = \varkappa\theta_{cxx} \qquad (x < 0, t > 0) \qquad (3)$$

$$\theta = T_w \qquad (x = 0) \qquad (4a)$$

$$\theta \to T_\infty \qquad (x \to \infty) \qquad (4b)$$

and

$$\theta = T_\infty \qquad (t = 0) \qquad (4c)$$

The velocity of migration of the interface between fluid and solid is proportional to the difference in the conductive heat flux across the wall and is

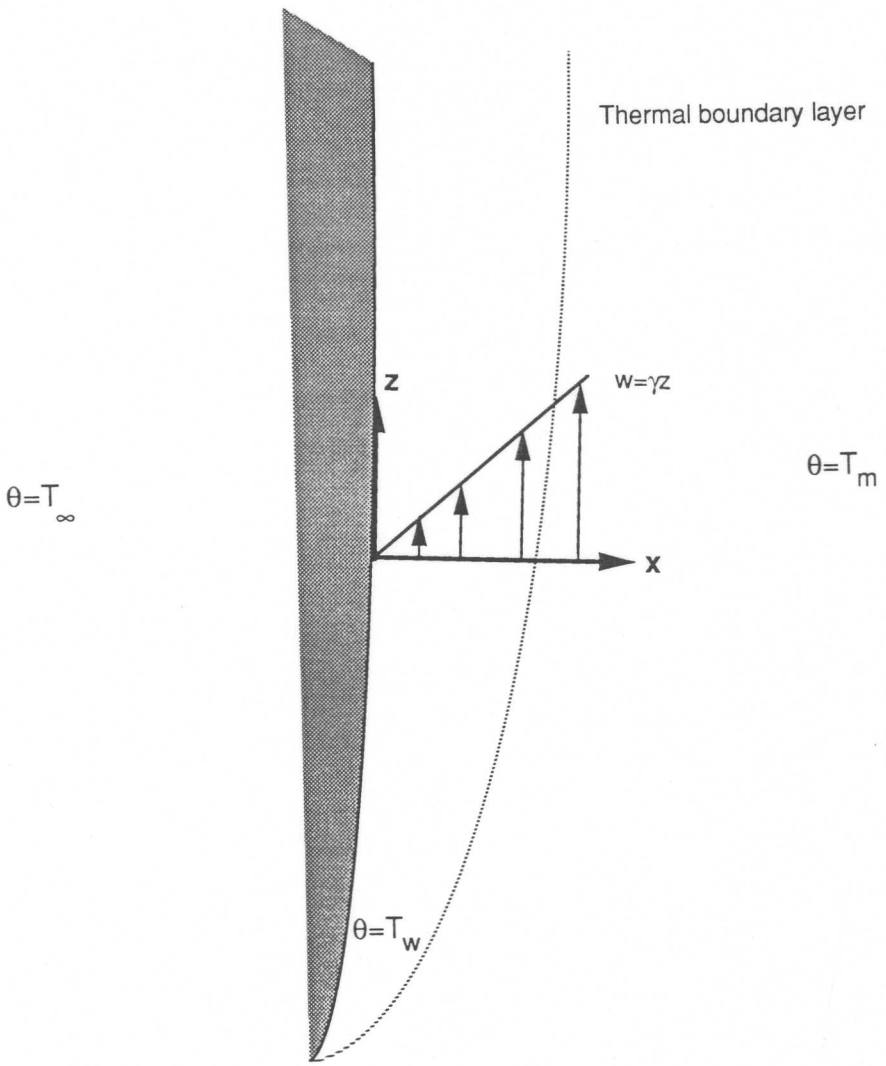

Figure 4. A sketch of the locally cartesian coordinate axes and the uniform shear flow at the wall

determined from

$$(L/c)v = -\varkappa[\theta_x(0+,z,t) - \theta_x(0-,z,t)] \quad (5)$$

where L is the latent heat of either solidification or melting, c is the specific heat and fluid and solid are assumed to have the same values for their thermal parameters.

The shear flow, which takes place at the edges of a two-dimensional channel of half-width $b(z,t)$ is driven by a pressure difference ΔP and results in a volume flow rate of $Q(t)$. These will be related by Poiseuille's Law (e.g., Bachelor, 1967), which implies both that

$$\Delta P = \frac{3}{2}\mu Q(t)\int_0^h b^{-3}(z,t)\,\mathrm{d}z \quad (6)$$

where μ is the dynamic viscosity, and that

$$\gamma(z,t) = \frac{3}{2}b^{-2}(z,t)Q(t) \quad (7)$$

Due to either solidification or melting at the walls, the half-width of the channel gradually changes according to

$$b(z,t) = b_i - \int_0^t v(z,t')\,\mathrm{d}t' \quad (8)$$

where b_i is the initially uniform half-width.

It is now instructive to introduce non-dimensional variables X, Z, T, V, ϑ and φ into

equations (1)–(5) by writing

$$x = (\varkappa/\gamma_i)^{1/2} X,\ z = (\varkappa/\gamma_i)^{1/2} Z,\ t = T/\gamma_i,$$
$$v = (\varkappa\gamma_i)^{1/2} V \qquad (9a\text{–}d)$$

$$\theta = T_w + (T_m - T_w)\vartheta \qquad (x < 0) \qquad (10a)$$

and

$$\theta = T_w + (T_w - T_\infty)\varphi \qquad (x < 0), \qquad (10b)$$

where $\gamma_i = b_i \Delta P/\mu h$ is the initial value of the shear. The resulting non-dimensional equations can then be expressed as

$$\vartheta_T - V\vartheta_X + \Gamma X \vartheta_Z = \vartheta_{XX} \qquad (X, T > 0) \quad (11)$$

$$\vartheta = 1 \qquad (Z = 0) \qquad (12a)$$

$$\vartheta = 0 \qquad (X = 0) \qquad (12b)$$

$$\vartheta \to 1 \qquad (X \to \infty) \qquad (12c)$$

$$\vartheta = 1 \qquad (T = 0) \qquad (12d)$$

$$\varphi_T - V\varphi_X = \varphi_{XX} \qquad (X < 0, T > 0) \qquad (13)$$

$$\varphi = 0 \qquad (X = 0) \qquad (14a)$$

$$\varphi \to -1 \qquad (X \to -\infty) \qquad (14b)$$

$$\varphi = -1 \qquad (T = 0) \qquad (14c)$$

and

$$V = -\left[S_m^{-1}\vartheta_X\,(0+, Z, T) - S_\infty^{-1}\varphi_X(0-, Z, T)\right] \qquad (15)$$

where

$$\Gamma = \gamma/\gamma_i \qquad (16)$$

is the ratio of the shear to its initial value,

$$S_m = L/c(T_m - T_w) \qquad (17)$$

is the Stefan number of the fluid and

$$S_\infty = L/c(T_w - T_\infty) \qquad (18)$$

is the Stefan number of the solid. These Stefan numbers are two of the dimensionless parameters that specify the behaviour of the flow. Physically, S_m represents the ratio of the latent heat of solidification to the heat released by the fluid on cooling from its initial or far-field value to the solidification temperature. Correspondingly, S_∞ represents the ratio of the latent heat of melting to the heat required to raise the solid from its initial or far-field temperature to the melting temperature.

Determination of the full solution of equations (11)–15) would be a formidable task, even numerically. Simplifications can be made, however, which ease the computational task and still permit an evaluation of the conditions under which the channel becomes blocked. They proceed by identifying two temporal regimes. During the first regime both fluid and solid are adjusting to the temperature at the wall T_w. During the subsequent regime, the continual supply of hot fluid transfers heat into the wall, while the solid continues to adjust to the wall temperature.

In the first regime, advection of heat by the flow is unimportant and the third term on the left-hand side of equation (11) can be neglected. (Formally the non-dimensional shear strength Γ is set equal to 0.) The resulting equations (11)–(15) have solutions in terms of the (non-dimensional) similarity variable

$$\xi = \frac{1}{2} XT^{-1/2} \qquad (19)$$

and can be written as

$$\vartheta = 1 - \frac{\operatorname{erfc}(\xi + \xi_0)}{\operatorname{erfc}\ \xi_0} \quad (\xi \geqslant 0) \qquad (20a)$$

$$\varphi = -1 + \frac{\operatorname{erfc}\{-(\xi + \xi_0)\}}{\operatorname{erfc}(-\xi_0)} \quad (\xi \leqslant 0) \qquad (20b)$$

where $\operatorname{erfc}(y)$ is the complementary error function of argument y, and

$$V = \xi_0 T^{-1/2} \qquad (20c)$$

on the condition that ξ_0 satisfies

$$\pi^{1/2}\xi_0 e^{\xi_0^2} = \left[\frac{1}{S_\infty \operatorname{erfc}(-\xi_0)} - \frac{1}{S_m \operatorname{erfc}\xi_0}\right] \qquad (21)$$

Equation (21) can be shown to have a positive solution, corresponding to solidification, if $S_m < S_\infty$ and a negative solution otherwise. Eigenvalue relationships of this form occur frequently in the solution of initial-value problems for the heat conduction equation, either with or without moving boundaries (Carslaw and Jaeger, 1959). The solution in both dimensional and non-dimensional form is sketched in Figure 5.

This solution, based on the neglect of advective processes, can be valid only in the early stages of the flow. After a time, advection in the fluid, as represented by the $\Gamma X \vartheta_Z$ term in equation (11), is balanced by conduction across the thin boundary layer at the wall, as represented by the ϑ_{XX} term. It seems reasonable to suppose that with further

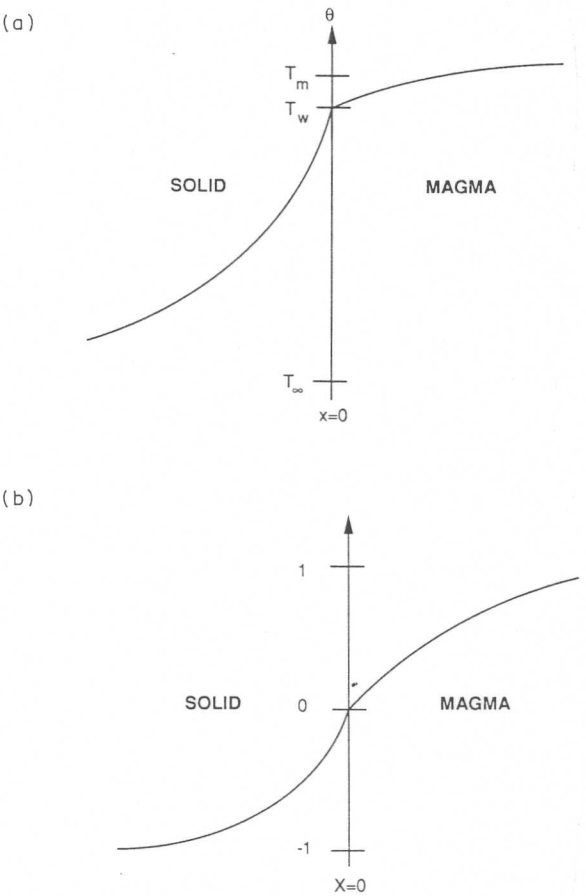

Figure 5. A sketch of the temperature profile in the magma and the solid in (a), dimensional terms, and (b) non-dimensional terms.

time, changes in the flow occur slowly and that hence ϑ_T can be neglected. The $-V\vartheta_X$ term in the boundary layer is now small compared with ϑ_{XX} and can be neglected also. This leaves, as the governing equation in the fluid,

$$\Gamma X\vartheta_Z = \vartheta_{XX} \qquad (X > 0) \tag{22}$$

and equations (12a–c) but of course not (12d). A more rigorous and detailed discussion of the validity of equation (22) is presented in Bruce (1989) along with fuller considerations of some of the subsequent approximations.

The form of equations (22) and (12a–c) suggest that a solution can be obtained in terms of the similarity variable

$$\eta = XZ^{-1/3} \tag{23}$$

Inserting equation (23) into (12a–c) and (22), we obtain

$$\vartheta_{\eta\eta} + \frac{1}{3}\Gamma\eta^2\vartheta_\eta = 0 \tag{24}$$

$$\vartheta = 0 \qquad (\eta = 0) \tag{25a}$$

$$\vartheta = 1 \qquad (\eta \to \infty) \tag{25b}$$

On the assumption that Γ is slowly varying, an assumption that only holds sufficiently far from the source of the flow, the solution to equations (24) and (25) is

$$\vartheta = 1 - P(\Gamma^{1/3}\eta/9^{1/3}) \tag{26}$$

where

$$P(u) = \int_u^\infty e^{-s^3}ds \Big| \int_0^\infty e^{-s^3}\,ds \tag{27a}$$

$$= 3\int_u^\infty e^{-s^3}\,ds \Big| \Gamma(1/3) \tag{27b}$$

and $\Gamma(1/3)$ is the gamma function of argument $1/3$.

The solution to equations (13)–(15) can be expressed in terms of the two independent variables ξ and

$$\tau = TZ^{-2/3} \tag{28}$$

Substituting equations (19) and (28) into (13)–(15), we obtain

$$4\tau\varphi_\tau = 2[\xi + K(\tau;Z)]\varphi_\xi + \varphi_{\xi\xi} \qquad (\xi < 0) \tag{29}$$

$$\varphi = 0 \qquad (\xi = 0) \tag{30a}$$

and

$$\varphi \to -1 \qquad (\xi \to -\infty), \tag{30b}$$

where

$$K(\tau;Z) \equiv VT^{1/2}$$

$$= \frac{1}{2}S_\infty^{-1}\varphi_\xi(\tau,0) - S_m^{-1}T^{1/2}\vartheta_x(0+,Z,T) \tag{31a,b}$$

Using equations (23), (26) and (27) to evaluate the last term in equation (31b), we see that

$$T^{1/2}\vartheta_X(0+,Z,T) = T^{1/2}Z^{-1/3}\vartheta_\eta(0) \tag{32a}$$

$$= -(\Gamma/9)^{1/3}P'(0)\tau^{1/2} \tag{32b}$$

where

$$P'(0) = -3/\Gamma(1/3) = -1.1198\ldots \tag{33a,b}$$

Since Z enters equations (29)–(31) only parametrically and we are primarily interested in the behaviour of the flow at the top of the wall,

at $Z = (\gamma_i/\varkappa)^{1/2}h = (b_i\,\Delta Ph/\varkappa\mu)^{1/2} \equiv Z_h$, it would be efficient if the system needed only to be solved at $Z = Z_h$. This can be done if $b(z,t)$, which appears in the integrand of

$$\Gamma(z,t) = hb^{-2}(z,t)\left[\int_0^h b^{-3}(z,t)\,\mathrm{d}z\right]^{-1}\Big/ b_i \quad (34)$$

is approximated as $b(h,t)$ on the argument that as the channel closes the dominant part of the integral comes from the region near $z = h$. In addition, the approximation is exact as $t = 0$ when the channel width is uniform. With this approximation

$$\Gamma(h,t) \equiv \Gamma_h \sim b(h,t)/b_i \quad (35a,b)$$

$$= 1 - b_i^{-1}\int_0^t v(h,t)\,\mathrm{d}t \quad (35c)$$

$$= 1 - (\varkappa/\gamma_i b_i^2)^{1/2}\int_0^T V(h,T)\,\mathrm{d}T \quad (35d)$$

To complete the specification of the problem, it remains only to determine the time domains of validity of the solutions in the flow represented by equations (20a) and (26). Given that equation (20a) is in terms of ξ and (26) is in terms of η, the demarcation between them will be in terms of the time-like variable $\tau = (\eta/2\xi)^2$. As τ increases, the conductive flux at the wall, $\xi = 0$, decreases—explicitly like $\tau^{-1.2}$. Over this time the convective flux calculated from equation (26) increases. We set the demarcation time between the domains of validity of the two solutions as the value of τ for which these two fluxes are equal at the top of the wall. Detailed calculations for the case $v \equiv 0$ in Bruce (1989) indicate that this is a reasonable approach. In addition, our subsequent results are not at all sensitive to this value. Denoting this value of τ by τ_d, we see from equations (19), (20a), (23), (26) and (27) that τ_d is given by

$$-\pi^{1/2}(\Gamma_h/9)^{1/3}\tau_d^{1.2}P'(0)\mathrm{e}^{\xi_0^2}\mathrm{erfc}\,\xi_0 = 1 \quad (36)$$

It follows from equations (9), (28) and (35c) that at $\tau = \tau_d$

$$\Gamma_h = 1 - 2\alpha\xi_0\tau_d^{1/2} \quad (37a)$$

where

$$\alpha = (\mu\varkappa h^2/\Delta Pb_i^4)^{1/3} \quad (38)$$

is the third of the three external parameters that specify the model. Physically, it represents the ratio of the initial width of the thermal boundary layer due to advection at the top of the dyke, given by the balance $\delta^2 = \varkappa h/\gamma_i\delta$, to the initial half-width b_i. For the model to be valid α must be less than 1. If α is too close to 1, as might happen for example if the dyke is too long or its initial width is too small, equation (36) does not have a solution and the dyke becomes blocked before advective effects become significant.

In the situation for which this does not occur, however, it remains only to solve for $\tau > \tau_d$

$$4\tau\varphi_\tau = 2[\xi + K(\tau; Z_h)]\varphi_\xi + \varphi_{\xi\xi} \qquad (\xi < 0, \tau > \tau_d), \quad (39)$$

$$\varphi = 0 \qquad (\xi = 0) \quad (40a)$$

$$\varphi \to -1 \qquad (\xi \to -\infty) \quad (40b)$$

and

$$\varphi = -1 + \frac{\mathrm{erfc}[-(\xi + \xi_0)]}{\mathrm{erfc}(-\xi_0)} \qquad (\tau = \tau_d) \quad (40c)$$

with

$$K(\tau; Z_h) = \frac{1}{2}S_\infty^{-1}\varphi_\xi(\tau, 0) + S_m^{-1}(\Gamma_h/9)^{1/3}P'(0)\tau^{1/2} \quad (41a)$$

and

$$\Gamma_h = 1 - \alpha\left[2\xi_0\tau_d^{1/2} + \int_{\tau_d}^{\tau} K(\tau; Z_h)\tau^{-1/2}\,\mathrm{d}\tau\right] \quad (41b)$$

where equation (41b) follows from (35d) on substitution of equations (20c) for $\tau < \tau_d$ and (31a) for $\tau > \tau_d$. The integro-differential system (39)–(41) represents the non-linear evolution of the non-dimensional temperature field at the top of the solid φ as a function of τ and ξ.

The system was solved by transforming the semi-infinite domain in ξ into [0,1), by setting $\xi = 2y/(y-1)$. A direct and robust numerical approach is to use a finite-difference formulation for the space-like variable y and integrate the resulting ordinary differential equations over τ. For the local part of the operator on the right-hand side of equation (39) we used the finite-difference scheme recommended by Sincovec and Madsen (1975) for parabolic equations; this is as compact as possible, as required for stability (see Hall and Watt, 1976, p. 210) and also conservative, as appropriate for a heat equation. To calculate the gradient at the boundary, on which the non-local term K depends, we used a one-sided four-point scheme, chosen on the basis of trials. For a parabolic system a stiff integrator is

required and the Gear variable-order/variable-step scheme was used in the NAG implementation D02EBF. This scheme uses generalized backward differences for the predictor, and modified Newton's method for the corrector. The step size was chosen to obtain sufficiently small local truncation error within a fixed number of iterations, and the order was chosen to maximize the step size within this contraint (see Hall and Watt, 1976, p. 154 *et seq.*). The number of points in the space dimension and the tolerance for the time integration were chosen so that the results were accurate to three significant figures.

The first, semi-implicit approach we used applied the Gear scheme only to the local operator and used a crude two-point predictor with an *ad hoc* corrector for $K(\tau; Z_h)$. However, because the total truncation error was not controlled, fully implicit solutions, applying Gear's scheme to the whole system, were also obtained using a software package that integrates a user-supplied discretization. Good agreement was found when the step length for the semi-implicit scheme was constrained to be small, by requesting a very stringent error bound on the local operator integration. The numerical routines were extensively checked by comparing the values obtained from them with those obtained by solving the system approximately using a different approach. Details of all such checks are presented in Bruce (1989).

The results of our calculations of the solutions to the full system are presented and discussed in the next section.

Results

The last section demonstrated how our two-dimensional model is controlled by the value of three external parameters: the Stefan number of the magma $S_m = L/c(T_m - T_w)$; the Stefan number of the surrounding country rock $S_\infty = L/c(T_w - T_\infty)$; and $\alpha = (\mu\varkappa h^2/\Delta P b_i^4)^{1/3}$. In our numerical calculations of equations (36)–(41), we used values of $c = 730$ J kg^{-1} °C^{-1}, $L = 8 \times 10^5$ J kg^{-1}, $\varkappa = 10^{-6}$ m^2 s^{-1}, $T_m = 1200$°C, $T_w = 1150$°C and $\mu = 100$ Pa s, which are representative of values for typical basaltic magmas (Huppert and Sparks, 1980, and references therein). The driving pressure was evaluated from the lithospheric overburden as $\Delta P/h = 2000$ nm^{-3} (Wilson and Head, 1981), with h taken as either 2 or 5 km. The depth interval 2–5 km corresponds to the top and bottom of active magma reservoirs in Hawaii, Iceland and the East Pacific Rise. It also corresponds approximately to the upper surface and the keel of dykes in the respective rift zones of these localities.

In a given volcanic system the remaining two variables T_∞ and b_i determine the course of successive eruptions. The value of T_∞ might vary between 0°C and 1150°C ($= T_w$) depending on the previous thermal history of the dyking zone. Using all these values, we find that $S_m = 22$, S_∞ ranges upwards from 1.05, which corresponds to cold country rock at 0°C, and that α can take on any positive value, though only if α is less than 1 are the details of the mathematical modelling valid.

On initiation of the flow of magma within the two-dimensional dyke at the commencement of the eruption, solidification in the boundary layers at the walls of the dyke results, unless the temperature in the surrounding country rock exceeds 1100°C, which will be a rare occurrence. For dykes less than a critical width the solidification continues until the dyke becomes blocked, which first occurs at the surface, and the eruption ceases. This form of evolution is sketched in Figure 6(a). For dykes initially broader than the critical width, before the solidification can close the channel the advected heat flux begins to melt back the solidified magma at the downstream end of the dyke. Melting continues along the whole length of the dyke, as sketched in Figure 6(b), and the width gradually increases, as long as the driving pressure is maintained.

The critical width is plotted as a function of the initial temperature of the crust of dykes 2 km and 5 km long in Figure 7(a) and the time taken for those dykes below the critical width to block is plotted in Figure 7(b) for a crustal temperature T_∞ of 100°C. The minimum width for an unblocked dyke as a function of the initial dyke width is plotted in Figure 7(c).

From the figure we see that large eruptions (initial widths greater than about 2 m) can always be sustained and that the length of the feeding dyke does not have a very large quantitative influence. For a small dyke, typified by those with an initial width less than a fraction of a metre, blocking generally occurs and does so within a matter of days. The behaviour of dykes of intermediate size depends quite critically on the initial

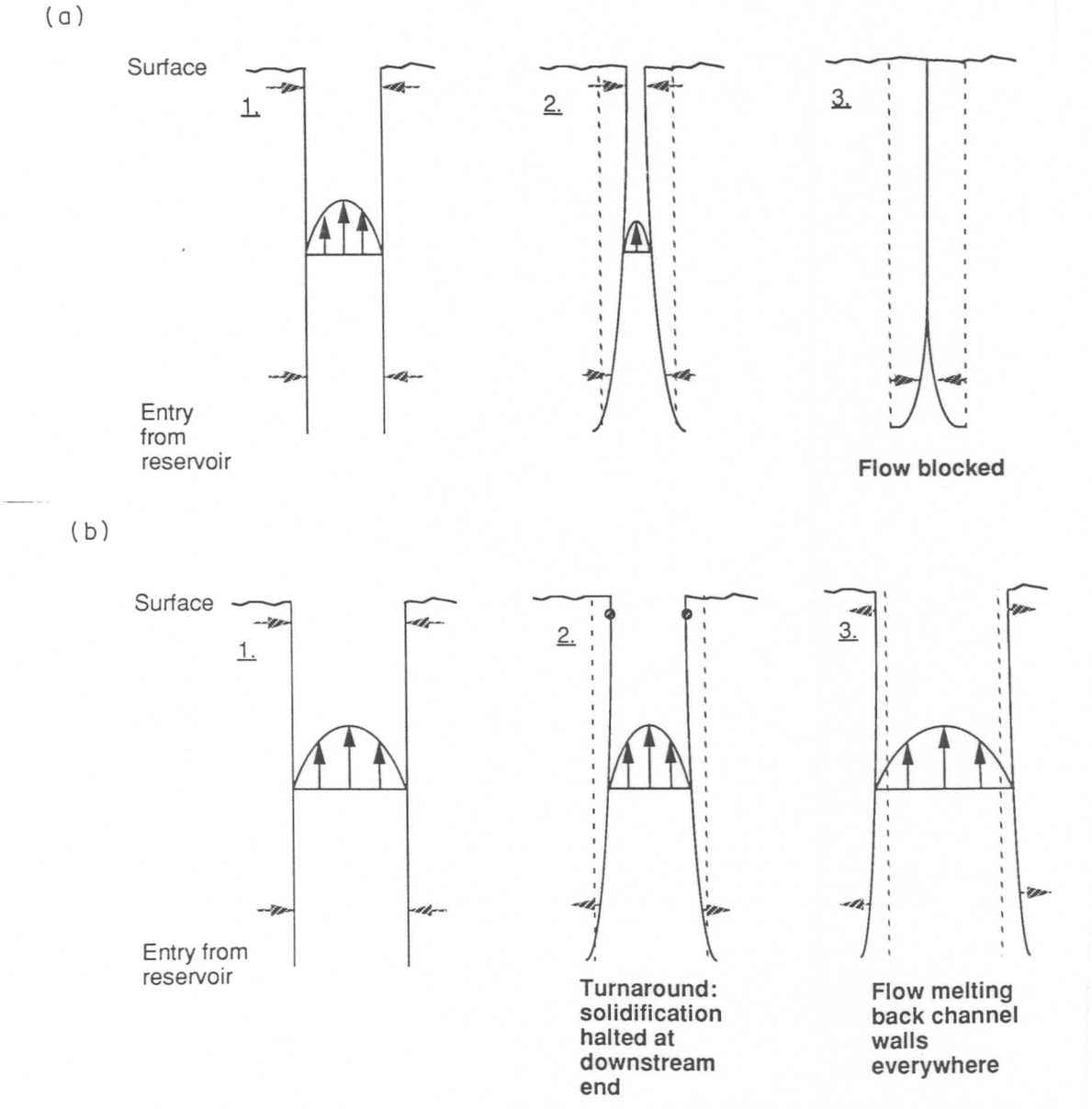

Figure 6. Sketches of the evolution in a two-dimensional dyke, showing either (a) the development to blocking, or (b) the development through turnaround and meltback

temperature of the crust. Eruptions from dykes emplaced in an initially warm environment have a greater tendency to persist. The variation in the value of T_∞ could be due to pre-heating of the country rock either by previous eruptive events or by hydrothermal circulation. Local warming by previous dyking events would take tens or more probably hundreds of years to decay by conduction, while the hydrothermal circulation may persist for variable periods up to maybe many tens of thousands of years depending on the volume and geometry of the magmatic heat source, country rock permeability and the kinetics of hydrothermal mineralization.

Three-dimensional effects

In addition to the influence of the crustal temperature in determining the evolution of a dyke with an initial width close to the critical value, there are

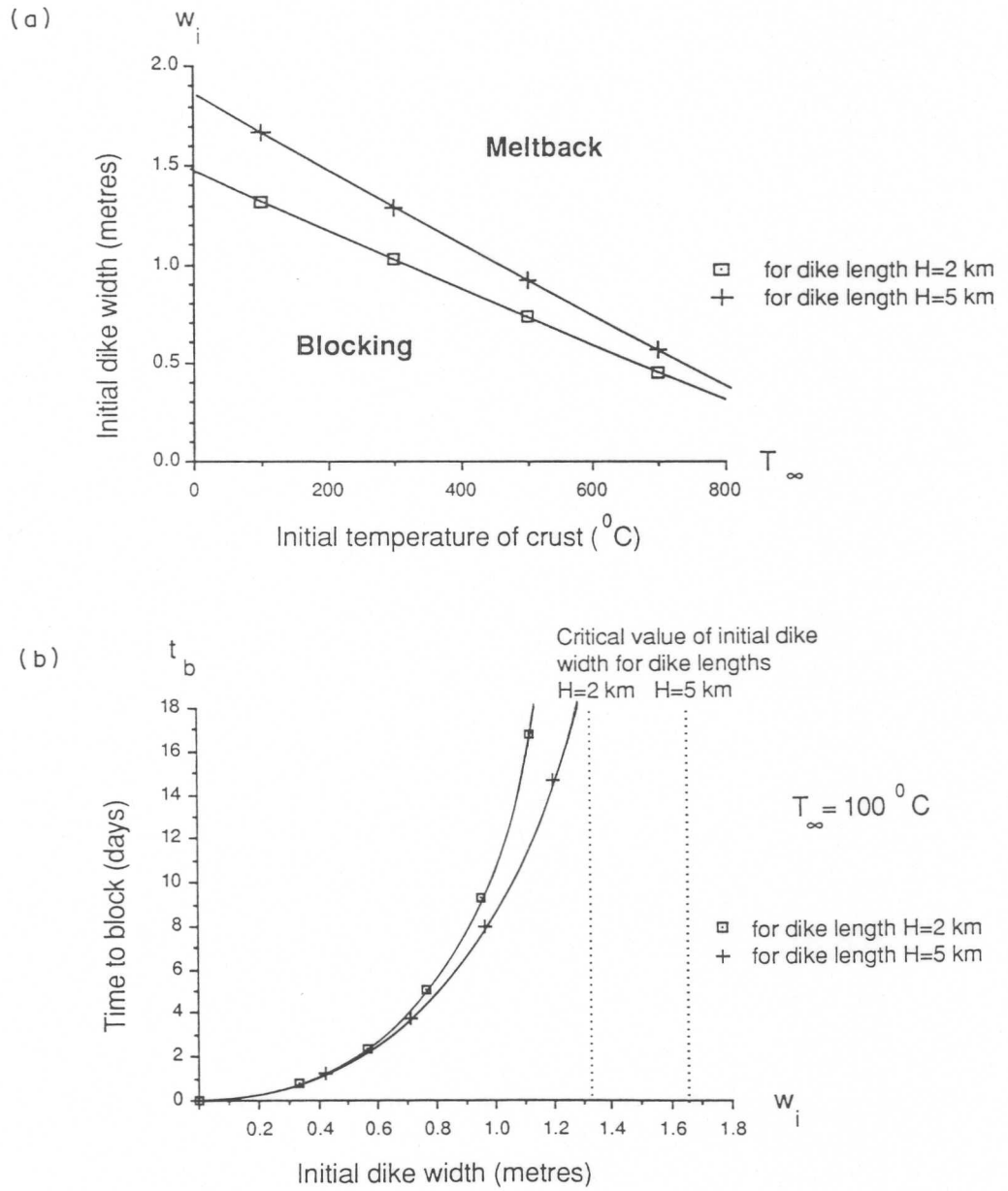

important three-dimensional effects. These occur because the magma that solidifies against the walls of the dyke constricts the flow, particularly at the downstream end of the dyke near the Earth's surface. This reduces the advected heat supply, which leads to further solidification and reduces the width of the dyke yet further. Correspondingly, melting the walls of the dyke increases the flow, provided the supply is maintained, and the increased advected heat flux results in additional melting. This positive feedback mechanism tends to maintain and even accelerate either solidification or melting. In a more realistic three-dimensional model of a dyke this feedback mechanism can result in solidification and melting occurring simultaneously in different parts of the surface fissure. The surface fissure and the dyke below it may have initially only small variations in width, as shown in Figure 8(a). These variations, however, may become significantly larger with

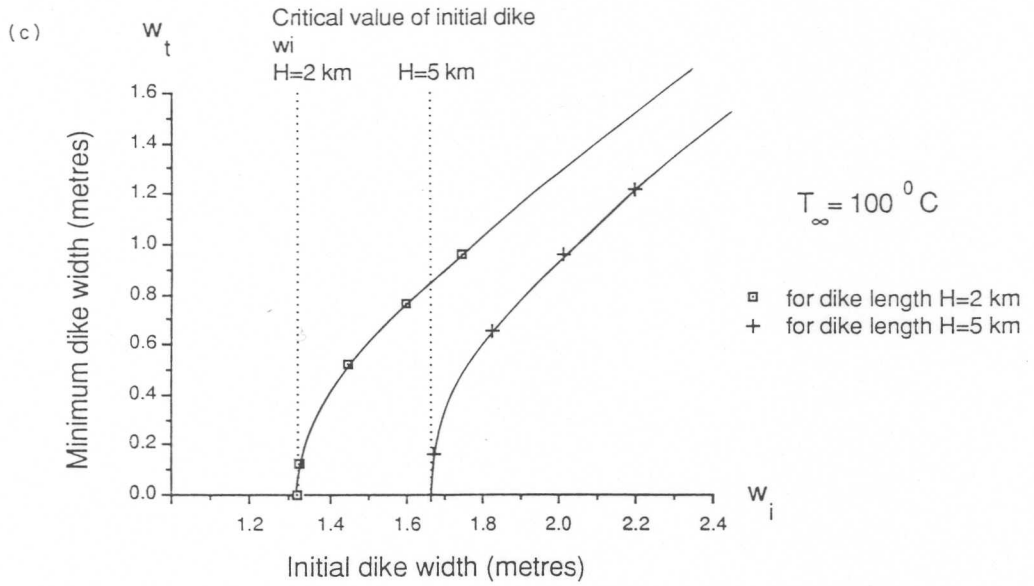

Figure 7. Numerical results of model, for parameter values given in text. (a) Regions of parameter space in which blocking or meltback are predicted. (b) Time for dyke to become blocked as a function of initial dyke width, for $T_\infty = 100^\circ C$. The time to block becomes infinite for initial widths approaching the critical value for meltback to occur. (c) Minimum width of dyke at turnaround as a function of initial dyke width, for $T = 100^\circ C$. The minimum dyke width at turnaround approaches zero as the initial width approaches the critical value for meltback to occur. For very large values of the initial dyke width, turnaround occurs before solidification has substantially changed the dyke width

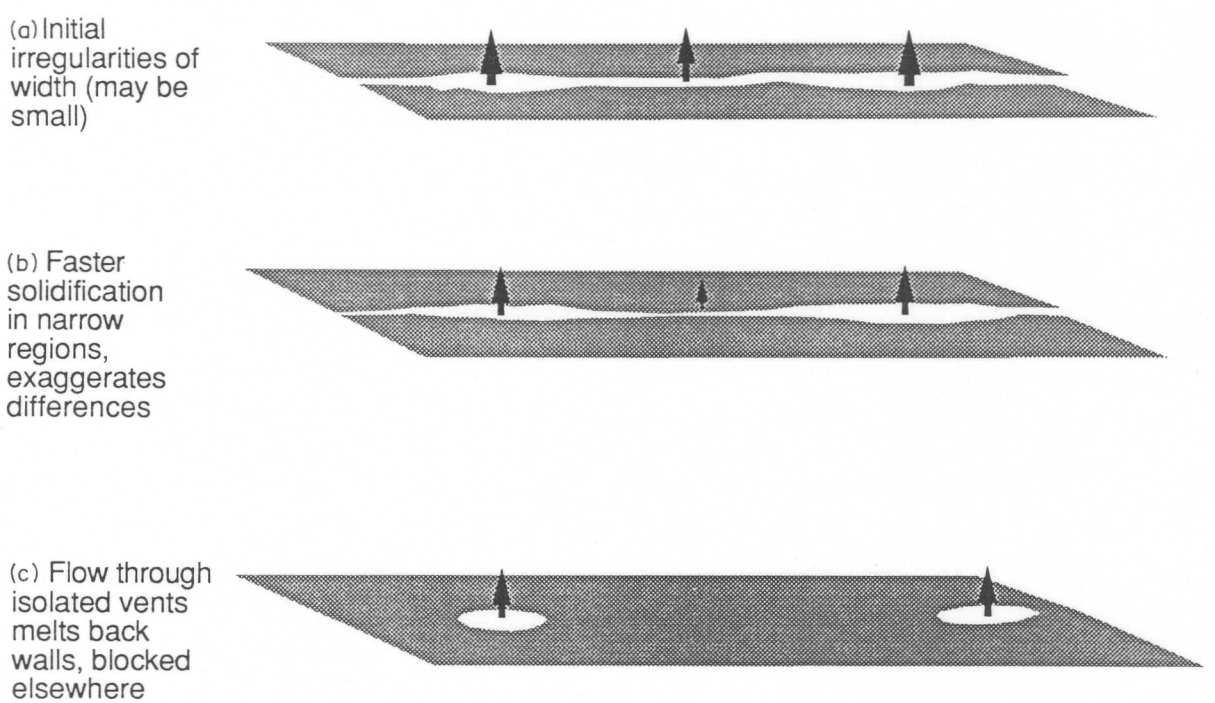

Figure 8. Sketches, not necessarily to scale, illustrating flow localization and subsequent development of a surface fissure over time

time, as was previously suggested qualitatively by McBirney (1984). This can occur because cross flows between sections of different initial widths will form as the flow up narrow sections encounters greater constrictions due to preferential solidification. The cross flows will further reduce the advected heat flux in the downstream portions of the narrow sections and increase it at the wider portions, thereby exaggerating small differences in the initial width of the dyke (Figure 8(b)).

In this way a fissure eruption can become confined within a matter of days to a number of isolated vents, from which magma continues to erupt, as depicted in Figure 8(c). The vents would continue to compete with each other for the supply of magma, though the interaction between vents becomes negligibly small if the vent separation exceeds the length of the dyke. This is because the drop in pressure associated with the sideways flow would then be comparable with the driving pressure. Since the localization process depends heavily on the operation of the feedback mechanism, isolated vents should only result from a fissure with an initial width sufficiently close to the critical value.

Conclusions

We have constructed a model that quantifies the thermal control processes generated by solidification or melting in a newly emplaced basaltic dyke feeding a fissure eruption. Heat supplied by the magma is both advected along the dyke and lost by conduction into the surrounding crust. For a small dyke, with an initial width less than a few tens of centimetres, conductive effects dominate and the magma continues to solidify against the walls until the dyke becomes blocked and the eruption ceases. Our calculations indicate that this typically occurs in a matter of days. For a large dyke, greater than a few metres in width, advective effects dominate and after an initial period of solidification the walls of the dyke are melted back. For dykes of intermediate width, three-dimensional effects are important and cross flows within the dyke can result in isolated vents forming while the length of fissure between the vents becomes blocked. The demarcation lines between the three forms of behaviour are fairly strong functions of the temperature of the surrounding country rock. An increase from 0°C to 500°C, for example, results in a decrease in the critical width by a factor of approximately two.

These predictions are broadly consistent with field observations of basaltic fissure eruptions. Macdonald and Abbot (1970), summarizing numerous eruptions on Hawaii, report that within a few days a long fissure either closes completely or evolves in such a way that the eruption continues from localized vents. Richter *et al.* (1970) describe a particular eruption that localized to a single vent within a day but then persisted for over a month. In all these eruptions the initial width of the dyke was typically less than 2 m. Anderson (1987) reports a succession of short-lived eruptions occurring in the same area that culminated in an eruption of much greater duration. We interpret this as the natural culmination of a series of eruptions through small dykes which became blocked as they lost heat and thereby warmed the surrounding crust. The temperature of the crust was finally raised sufficiently to allow the advected heat supply to suffice for the eruption to persist.

Acknowledgements

We are grateful to our colleagues R.C. Kerr, J.R. Lister, R.S.J. Sparks, A.W. Woods and M.G. Worster with whom we have had many stimulating discussions concerning the material of this paper. Considerable improvements of the presentation were kindly suggested to us by M.P. Ryan, who acted very efficiently throughout the preparation of this volume and imaginatively supplied us with the photographs that make up Figures 1 and 2. The research of PMB was supported by an NERC studentship. HEH is supported by a grant from the BP Venture Research Unit.

References

Anderson, I. (1987). Volcanoes in paradise. *New Scientist*, **1567**, 50–54.

Batchelor, G.K. (1967). *An Introduction to Fluid Dynamics*. Cambridge University Press, Cambridge, 615 pp.

Björnsson, A., Johnsen, G., Sigurdsson, S., Thorbergsson, G., and Tryggvason, E. (1979). Rifting of the plate boundary in north Iceland 1975–1978. *J. Geophys. Res.*, **84**, 3029–3038.

Brandeis, G. and Jaupart, C. (1986). On the interaction between convection and crystallization in cooling

magma chambers. *Earth Planet. Sci. Lett.*, **77**, 345–361.

Bruce, P.M. (1989). *Thermal convection within the Earth's crust*. PhD Dissertation, University of Cambridge, 169 pp.

Carslaw, H.S. and Jaeger, J.C. (1959). *Conduction of Heat in Solids*. Oxford University Press, Oxford, 510 pp.

Delaney, P.T. (1982). Rapid intrusion of magma into wet rock: groundwater flow due to pore pressure increases. *J. Geophys. Res.*, **87**, 7739–7756.

Delaney, P.T. and Pollard, D.D. (1982). Solidification of basaltic magma during flow in a dike. *Am. J. Sci.*, **282**, 856–885.

Hall, G. and Watt, J.M. (eds) (1976). *Modern Numerical Methods for Ordinary Differential Equations*. Clarendon Press, Oxford, 336 pp.

Hardee, H.C. and Larson, D.W. (1977). Viscous dissipation effects in magma conduits. *J. Volcanol. Geotherm. Res.*, **2**, 299–308.

Huppert, H.E. (1989). Phase changes following the initiation of a hot turbulent flow over a cold solid surface. *J. Fluid Mech.*, **198**, 293–319.

Huppert, H.E. and Sparks, R.S.J. (1980). The fluid dynamics of a basaltic magma chamber replenished by influx of hot, dense ultrabasic magma. *Contrib. Mineral. Petrol.*, **75**, 279–289.

Jaeger, J.C. (1968). Cooling ad solidification of igneous rocks. In: Hess, H. H. and Poldervaart, A. (eds) *Basalts: the Poldervaart Treatise on Rocks of Basaltic Composition*. Interscience, New York, pp. 503–536.

Lister, J.R. (1990). Buoyancy-driven fluid fracture: the effects of material toughness and of low-viscosity precursors. *J. Fluid Mech.*, in press.

McBirney, A.R. (1984). *Igneous Petrology*. Freeman, Cooper and Company, p. 56.

McBirney, A.R. and Murase, T. (1984). Rheological properties of magmas. *Ann. Rev. Earth Planet Sci.*, **12**, 337–357.

Macdonald, G.A. and Abbot, A.T. (1970). *Volcanoes in the Sea*. University of Hawaii Press, Honolulu.

Richter, D.H., Eaton, J.P., Murata, K.J., Ault, W.A., and Krivoy, H.L. (1970). Chronological narrative of the 1955–1960 eruption of Kilauea volcano, Hawaii, *U.S. Geol. Surv. Prof. Pap. 537-E*, pp. 1–73.

Ryan, M.P. and Blevins, J.Y.K. (1987). The viscosity of synthetic and natural silicate melts and glasses at high temperatures at 1 bar (10^5 pascals) pressure and at higher pressures. *U.S. Geol. Surv. Bull.*, **1765**, 455–457.

Sincovec, R.M. and Madsen, N.K. (1975). Software for nonlinear partial differential equations. *A.C.M. Trans. Math. Software*, **1**, 232–260.

Spence, D.A. and Sharp, P. (1985). Self-similar solutions for elastohydrodynamic cavity flow. *Proc. R. Soc. London, Ser. A*, **400**, 289–313.

Thorarinsson, S. (1969). The Lakagigar eruption of 1783. *Bull. Volcanol*, **33**, 910–929.

Thorarinsson, S., Steinthórsson, S., Einarsson, Th., Kristmannsdóttir, H., and Oskarsson, N. (1973). The eruption on Heimay, Iceland. *Nature*, **241**, 372–375.

Wilson, L. and Head, J.W. (1981). Ascent and eruption of basaltic magma on the earth and moon. *J. Geophys. Res.*, **86**, 2971–3001.

Figure 1. (a) A series of eruptive fissures, arranged in an en echelon fashion, feeding an immense lava flow-field in the northeast rift zone of Mauna Loa volcano, Hawaii. Laminar flow in the dyke erupts as a turbulent curtain of fire with a maximum height that approaches 75 m. (Official US Geological Survey photo by J.P. Lockwood, 6 July, 1975.) (b) At least seven en echelon fissure segments are seen erupting simultaneously in the northeast rift zone of Mauna Loa volcano, Hawaii and producing lava that is flowing into the saddle that lies between Mauna Loa and Mauna Kea. (Official US Geological Survey photo by J.P. Lockwood, 6 July, 1975)

Figure 1. (a) A series of eruptive fissures, arranged in an en echelon fashion, feeding an immense lava flow-field in the northeast rift zone of Mauna Loa volcano, Hawaii. Laminar flow in the dyke erupts as a turbulent curtain of fire with a maximum height that approaches 75 m. (Official US Geological Survey photo by J.P. Lockwood, 6 July, 1975.) (b) At least seven en echelon fissure segments are seen erupting simultaneously in the northeast rift zone of Mauna Loa volcano, Hawaii and producing lava that is flowing into the saddle that lies between Mauna Loa and Mauna Kea. (Official US Geological Survey photo by J.P. Lockwood, 6 July, 1975)

Figure 2. (a) A turbulent curtain of fire above eruptive fissures near the current Pu'u O'o vent site. (Photograph by J. Griggs, US Geological Survey in February, 1983. Reproduced with permission.) (b) A series of eruptive fissures in the east rift zone of Kilauea volcano, Hawaii. Subsequent to the activity pictured here the eruption localized to a single vent at Pu'u O'o. (Photograph by J. Griggs, US Geological Survey in February, 1983. Reproduced with permission)

Figure 2. (a) A turbulent curtain of fire above eruptive fissures near the current Pu'u O'o vent site. (Photograph by J. Griggs, US Geological Survey in February, 1983. Reproduced with permission.) (b) A series of eruptive fissures in the east rift zone of Kilauea volcano, Hawaii. Subsequent to the activity pictured here the eruption localized to a single vent at Pu'u O'o. (Photograph by J. Griggs, US Geological Survey in February, 1983. Reproduced with permission)

CAPTIONS TO COLOUR PLATES IN CHAPTER 6